

# Oleate vesicle template route to silver nanowires†

Xuchuan Jiang, Yi Xie,\* Jun Lu, Liying Zhu, Wei He and Yitai Qian

Structure Research Lab. and Lab. of Nanochemistry & Nanomaterials, University of Science & Technology of China, Hefei, Anhui, 230026, P. R. China. E-mail: yxie@ustc.edu.cn

Received 20th April 2001, Accepted 26th April 2001  
 First published as an Advance Article on the web 10th May 2001

Silver nanowires with sizes of  $\sim 35 \text{ nm} \times 300 \text{ nm}$  are synthesized in a lamellar liquid crystalline alignment of oleate vesicles *via* UV irradiation under ambient conditions. The passivation of oleate amphiphiles on the surface of silver nanoparticles is utilized for the nucleation and directional growth of silver nanowires. Increasing silver nanoparticle size leads to a strong red shifting of the surface plasmon absorption band from 395 to 500 nm. The proposed formation mechanism of silver nanowires and crosslinking processes are discussed.

Nanostructured noble metallic clusters, particularly one-dimensional (1D) nanomaterials, are currently the focus of much attention due to their special properties.<sup>1</sup> Such nanoscale materials have potential applications in both mesoscopic research and development of nanodevices. Nanoclusters of noble metals can be used as catalysts or as magnetic, electronic or photonic materials.<sup>2–7</sup> In recent years, many methods, particularly template-assisted methods, have been developed to synthesize noble metallic 1D nanomaterials such as carbon nanotubes,<sup>8,9</sup> these include electrodeposition in nanopores of anodized alumina and polymer templates,<sup>10</sup> block copolymers,<sup>11</sup> Langmuir–Blodgett (LB) films,<sup>12,13</sup> DNA molecule templates,<sup>14</sup> and sodium dodecyl sulfate (SDS) micelles–copolymer gel templates.<sup>15</sup> Recent developments on the theme of “vesicle templating” are highlighted. This theme has attracted attention as, in principle, it represents a unique opportunity in the morphological construction of materials by direct imprinting of the shape and texture of the template. Hubert *et al.*<sup>16</sup> reported a vesicle templating route to construct submicrometer hollow polymer particles. Here we report a synthesis route to construct a 1D silver nanostructure in a lamellar liquid crystalline array of oleate vesicles by UV irradiation. This approach is based on a novel sodium oleate/1-octanol/water gel phase with a liquid crystalline array consisting of monodisperse and unilamellar vesicles with diameter of  $\sim 40 \text{ nm}$ .<sup>17</sup>

In a typical procedure, sodium oleate is prepared by titration of oleic acid with sodium hydroxide in ethanol according to the literature method.<sup>18</sup> All the chemical reagents used here are analytically pure. The ternary system of sodium oleate/1-octanol/water is formed with a molar ratio of 2:1 for octanol/oleate and a total concentration of 5.0 wt% for amphiphiles. In the following process,  $0.02 \text{ mol dm}^{-3}$   $\text{AgNO}_3$  solution was substituted for the deionized water. The mixed system of 50 ml total volume was stirred for 2 h at room temperature and it became transparent, isotropic and viscous, consistent with the literature report.<sup>17</sup> The mixture was irradiated with a 40 W,

column-like, low-pressure mercury lamp ( $\lambda = 253.7 \text{ nm}$ ). After 48 h UV irradiation, the dark brown precipitate was filtered off, washed with water and ethanol *via* sonication, and finally dried in vacuum at  $30^\circ \text{C}$  for 4 h.

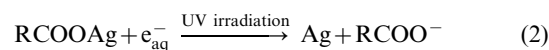
Oily streaky and clover-leaf textures are observed under a polarized optical microscope (POM), which indicates a lamellar liquid crystalline alignment of vesicles.<sup>19</sup> The texture changes only a little upon formation of the 1D silver nanostructured particles upon UV irradiation. The low-angle X-ray diffraction (XRD) patterns‡ indicate that the oleate vesicle system is in a lamellar array, with the interlayer spacing distance estimated as *ca.* 4.50 nm in the  $2\theta$  range  $2\text{--}15^\circ$ .

All the XRD reflections can be indexed to a cubic Ag phase with the cell parameter  $a = 4.0805 \text{ \AA}$ , which is consistent with the reported data (JCPDS Cards File, 4-783). The XRD pattern of the silver nanoparticles exhibits only four peaks in the  $2\theta$  range  $10\text{--}65^\circ$ , which can be assigned to the 100, 110, 111 and 200 diffraction planes, respectively, for the cubic silver phase. The as-prepared nanoparticles are identified as pure-phase silver by energy dispersive X-ray (EDX) analysis.

The binding energies obtained in X-ray photoelectron spectra (XPS)§ analysis were corrected for specimen charging by referencing the C 1s peak to 284.80 eV. The binding energy value is 368.1 eV for Ag  $3d_{5/2}$  and the kinetic energy value is 895.4 eV for Ag MNN, respectively, which are in good agreement with the literature values.<sup>20</sup>

The morphology and size of the silver nanowires¶ were observed by transmission electron microscopy (TEM) and are shown in Fig. 1, the crosslinking Ag nanowires are  $\sim 30 \text{ nm} \times 300 \text{ nm}$  in size after 48 h UV irradiation. Meanwhile, individual, nearly spherical Ag nanoparticles are *ca.* 9 nm in diameter and some Ag nanorods with diameter of  $\sim 30 \text{ nm}$  were observed after 6 and 24 h UV irradiation, respectively. With increasing UV irradiation time, the aggregation of Ag nanoparticles is evident. The diffraction spots in an electron diffraction image show that the product crystallizes well under ambient conditions. The interplanar distance of the  $\{110\}$  lattice fringes is *ca.* 2.86 Å as observed in a high-resolution transmission electron microscopy (HRTEM) image.

Here it seems relevant to discuss the growth process of the Ag nanowires. The possible reactions are given by eqns. (1) and (2),



where R represents the  $\text{CH}_3(\text{CH}_2)_7\text{CH}=\text{CH}(\text{CH}_2)_7-$  group. From eqns. (1) and (2),  $\text{Ag}^+$  ions can be reduced by hydrated electrons generated by UV irradiation,<sup>21</sup> which is also suggested by the observation of the ternary sodium oleate/

†Electronic supplementary information (ESI) available: Fig. S1: low-angle XRD patterns of the ternary solution prior to and after UV irradiation, Fig. S2: XRD and EDX patterns of the silver nanocomposite, Fig. S3: TEM images for the silver nanostructures. See <http://www.rsc.org/suppdata/jm/b1/b103718h/>

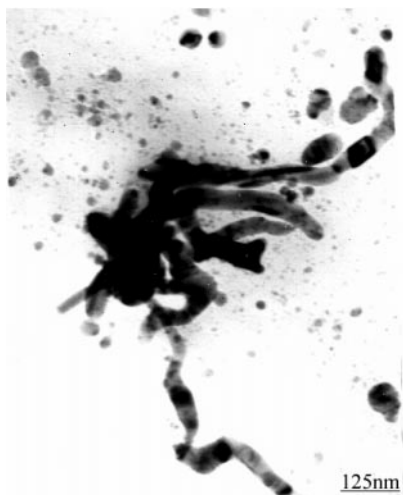
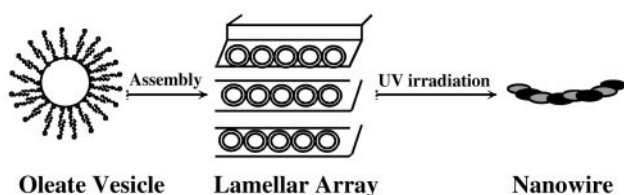


**Fig. 1** TEM image of silver nanowires with size of  $\sim 30 \text{ nm} \times 300 \text{ nm}$ .

1-octanol/aqueous  $\text{AgNO}_3$  system changing from transparent to dark brown as the reaction proceeds. By contrast, when the same ternary system was exposed to normal light without UV irradiation, the color of the mixture turned light brown after a month at room temperature, and only spherical Ag particles were obtained. This result indicates that UV irradiation promotes the reduction of  $\text{Ag}^+$  and formation of Ag nanoparticles.

Scheme 1 illustrates the assembly processes of silver nanoparticles in the lamellar arrays of oleate vesicles. The Ag nuclei form and grow as spherical particles in oleate vesicles through the reduction reaction upon UV irradiation. The formation of silver nanowires is expected if the following two conditions are fulfilled: (i) factors promoting growth of Ag particles in a particular direction, *i.e.*  $\text{Ag}^+$  reduction at a definite site on the growing silver particle, and (ii) diffusion limitations on  $\text{Ag}^+$  ions in the system. In this case, the “water-pool” of the vesicles provides a micro-reactor for silver, while the lamellar arrays of oleate vesicles are favorable for epitaxial growth within a single layer. Association between end groups of amphiphiles results in the crosslinking of the particles being confined to the single-layer region of the liquid crystal due to oleate intercalation and surface exchange reactions.<sup>22</sup> Torigoe and Esumi<sup>15</sup> speculated in a related system that adsorbed SDS and polymer on Pd particles induce preferential growth of the Pd particles at particular surfaces with low surface excess energy. In the present work, it is tentatively assumed that hydrophilic headgroups preferentially passivate the surfaces of silver nuclei, resulting in the growth of silver nanowires along the *c*-axis. Analogously to the formation of  $\text{BaCO}_3$  nanowires in  $\text{C}_{12}\text{E}_4$  (tetraethylene glycol monododecyl ether) reverse micelles,<sup>23</sup> tiny amorphous silver particles, developed from the primary nuclei, aggregate into wires in a directional manner, with desorption of the amphiphile and silver crystallization. Although such a proposed mechanism remains to be confirmed by more detailed investigations, it is evident that the silver nanowires are formed by aggregation rather than the layer-by-layer growth proposed for the zincophosphate sodalite in AOT



**Scheme 1** Illustration of the assembly processes of silver nanowires in the lamellar array of oleate vesicles under UV irradiation.

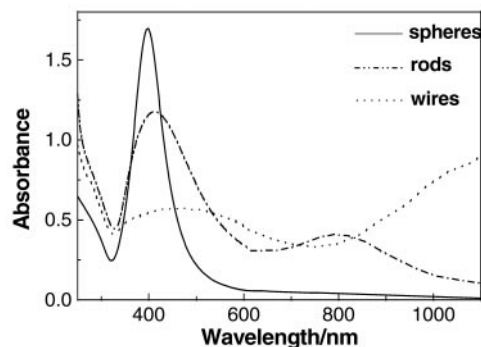


**Fig. 2** UV-vis absorption spectra of silver spherical particles (solid line), rods (dash-dot line) and wires (dotted line).

[bis(2-ethylhexyl)sulfosuccinate] reverse micelles.<sup>24</sup> It seems that the interactions between the amphiphiles of oleate vesicles exert some sort of directing influence on the growth of the silver nanowires.

The UV-vis absorption spectra of Ag nanostructures are shown in Fig. 2. The maximum absorption at 395 nm correlates with the size of the small spherical Ag particles, similarly to reported data in citrate solution.<sup>25</sup> Research has shown that the energy of the surface plasmon band is sensitive to various factors, including particle size, shape, surrounding media and interparticle interactions.<sup>10,26–28</sup> The changeover of silver nanostructure from spherical to rod-like shapes leads to a splitting from an original single absorption band to two absorption bands which separate with increasing aspect ratio.<sup>27</sup> As shown in Fig. 2, the optical properties of the dispersion indeed change markedly with aspect ratio. Instead of a single adsorption maximum seen for the spherical silver particles, two maxima are found for the rods and wires. The absorption maximum for silver in the range 395–500 nm is attributed to the transverse plasmon resonance,<sup>29</sup> while the second peak in the near infrared is attributed to the longitudinal plasmon resonance for rods or wires.<sup>30</sup> Here, the system containing Ag nanostructures with different sizes and orientations, shows overlap of the absorption bands which results in a broadening of the absorption bands and red shifting of the transverse plasmon resonance,<sup>31</sup> which is similar to the absorption spectra of Au rods in templates.<sup>10</sup>

In summary, a novel vesicle templating route to construct silver nanowires by UV irradiation is reported. The nucleation and growth of silver nanoparticles are controlled by the size of the oleate vesicles. The amphiphile passivation on the silver surface plays an important role in the aggregation of silver nanoparticles. This work provides a unique way to tailor the shape and size of metallic nanoparticles through alignment of vesicles.

## Acknowledgements

Financial support from the Chinese National Foundation of Natural Science Research and the China Ministry of Education is gratefully acknowledged.

## Notes and references

‡X-Ray powder diffraction (XRD) patterns were recorded on a Japan Rigaku D/max- $\gamma$  rotation anode X-ray diffractometer, using Ni-filtered  $\text{CuK}_\alpha$  radiation ( $\lambda = 1.54178 \text{ \AA}$ ), with a scanning rate of  $0.05^\circ \text{ s}^{-1}$ .

§X-Ray photoelectron (XPS) spectra at an energy resolution of 1.0 eV were recorded on an ESCALab MK II instrument with  $\text{MgK}_\alpha$  radiation ( $h\nu = 1253.6 \text{ eV}$ ) as the excitation source.

¶Morphology and size of silver nanowires were observed by transmission electron microscopy (TEM) images, along with energy dispersion X-ray (EDX) analysis, which were taken on a Hitachi H-800 transmission electron microscope. High-resolution electron microscopy

(HRTEM) images of the as-prepared product were taken on a JEOL-2010 transmission electron microscope with an acceleration voltage of 200 kV.

UV-vis absorption spectra were recorded on a UV-vis spectrophotometer (Specord 200) in the wavelength range 190–1100 nm (Analytik Jena GmbH, Germany).

- 1 A. M. Rao, E. Richter, S. Bandow, B. Chase, P. C. Eklund, K. A. Williams, S. Fang, K. R. Subbaswamy, M. Menon, A. Thess, R. E. Smalley, G. Dresselhaus and M. S. Dresselhaus, *Science*, 1997, **275**, 187.
- 2 N. R. Jana, Z. L. Wang and T. Pal, *Langmuir*, 2000, **16**, 2457.
- 3 J. Crangel and W. R. Scott, *J. Appl. Phys.*, 1965, **36**, 921.
- 4 L. N. Lewis, *Chem. Rev.*, 1993, **93**, 2693.
- 5 N. Roost, L. Ackermann and G. Pacchioni, *Chem. Phys. Lett.*, 1992, **93**, 94.
- 6 A. Henglein, *Chem. Rev.*, 1989, **89**, 1861.
- 7 G. D. Stucky and J. E. MacDougall, *Science*, 1990, **247**, 669.
- 8 D. T. Colbert, J. Zhang, S. M. McClure, P. Nikolaev, Z. Chen, J. H. Hafner, D. W. Owens, P. G. Kotula, C. B. Carter, J. H. Weaver, A. G. Rinzler and R. E. Smalley, *Science*, 1994, **266**, 1218.
- 9 J. Sloan, D. M. Wright, H.-G. Woo, S. Bailey, G. Brown, A. P. E. York, K. S. Coleman, J. L. Hutchison and M. L. H. Green, *Chem. Commun.*, 1999, 699; S. Fullam, D. Cottell, H. Rensmo and D. Fitzmaurice, *Adv. Mater.*, 2000, **12**, 1430.
- 10 B. M. I. van der Zande, M. R. Böhmer, L. G. J. Fokkink and C. Schönenberger, *J. Phys. Chem. B*, 1997, **101**, 852; B. M. I. van der Zande, L. Pagès, R. A. M. Hikmet and A. van Blaaderen, *J. Phys. Chem. B*, 1999, **103**, 5761; B. M. I. van der Zande, M. R. Böhmer, L. G. J. Fokkink and C. Schönenberger, *Langmuir*, 2000, **16**, 451.
- 11 R. W. Zehner, W. A. Lopes, T. L. Morkved, H. Jaeger and L. R. Sita, *Langmuir*, 1998, **14**, 242.
- 12 S. W. Chen, *Adv. Mater.*, 2000, **12**, 186.
- 13 E. Braun, Y. Eichen, U. Sivan and G. BenYoseph, *Nature*, 1998, **391**, 775.
- 14 S.-W. Chung, G. Markovich and J. R. Heath, *J. Phys. Chem. B*, 1998, **102**, 6685.
- 15 K. Torigoe and K. Esumi, *Langmuir*, 1995, **11**, 4199.
- 16 D. H. W. Hubert, M. Jung and A. L. German, *Adv. Mater.*, 2000, **12**, 1291.
- 17 M. Gradzielski, M. Bergmeier, M. Müller and H. Hoffmann, *J. Phys. Chem. B*, 1997, **101**, 1719; M. Gradzielski, M. Müller, M. Bergmeier, H. Hoffmann and E. Hoinkis, *J. Phys. Chem., B*, 1999, **103**, 1416.
- 18 B. D. Flockhart and H. Graham, *J. Colloid Sci.*, 1953, **8**, 105.
- 19 F. B. Rosevear, *J. Am. Oil Chem. Soc.*, 1954, **31**, 628.
- 20 C. D. Wagner, W. W. Riggs, L. E. Davis, J. F. Moulder and G. E. Muilenberg, *Handbook of X-Ray Photoelectron Spectroscopy*, Perkin-Elmer Corporation, Physical Electronics Division, Eden Prairie, MN, USA, 1979.
- 21 A. J. Swallow, *Radiation Chemistry of Organic Compounds*, Pergamon Press, Oxford, 1960.
- 22 M. J. Hostetler, A. C. Templeton and R. W. Murray, *Langmuir*, 1999, **15**, 3782.
- 23 L. M. Qi, J. M. Ma, H. M. Cheng and Z. G. Zhao, *J. Phys. Chem. B*, 1997, **101**, 3460.
- 24 K. S. N. Reddy, L. M. Salvati, P. K. Dutta, P. B. Abel, K. I. Suh and R. R. Ansari, *J. Phys. Chem.*, 1996, **100**, 9870.
- 25 A. Henglein and M. Giersig, *J. Phys. Chem. B*, 1999, **103**, 9533.
- 26 M. Kerker, *The Scattering of Light and other Electromagnetic Radiation*, Academic Press, New York, 1969.
- 27 C. F. Bohren and D. R. Huffmann, *Absorption and Scattering of Light by Small Particles*, Wiley, New York, 1983, ch. 12.
- 28 S. Underwood and P. Mulvaney, *Langmuir*, 1994, **10**, 3427.
- 29 C. A. Foss, G. L. Hornyak, J. A. Stocket and C. R. Martin, *J. Phys. Chem.*, 1994, **98**, 2963.
- 30 H. H. Huang, X. P. Ni, G. L. Loy, C. H. Chew, K. L. Tan, F. C. Loh, J. F. Deng and G. Q. Xu, *Langmuir*, 1996, **12**, 909.
- 31 C. R. Berry and D. C. Skillman, *J. Photogr. Sci.*, 1969, **17**, 145.